**RESEARCH ARTICLE**

**Key Points:**

- Glacier equilibrium line altitude (ELA) is more sensitive to precession than obliquity, unlike positive degree days
- The results were sensitive to how temperature was simulated in each climate model
- Ablation was more important than precipitation in determining ELA anomalies

**Correspondence to:**

G. R. O'Neill,
grainne.oneill@rutgers.edu

# Climate Model Simulations of the Effects of Orbital Parameters on Glacier Equilibrium Line Altitude

**G. R. O'Neill[1]** ⬤ and **A. J. Broccoli[1]** ⬤

[1]Department of Environmental Sciences and Institute of Earth, Ocean, and Atmospheric Sciences, Rutgers University, New Brunswick, NJ, USA

**Abstract** The effects of obliquity and precession on conditions favorable for Northern Hemisphere glaciation are explored using an energy balance and mass balance model of equilibrium line altitude (ELA), the height on a glacier where accumulation and ablation are in balance annually. Climate forcing for the ELA model is obtained from idealized single-forcing orbital simulations with two atm-ocean general circulation models, Geophysical Fluid Dynamics Laboratory (GFDL) CM2.1 and National Center for Atmospheric Research (NCAR) Community Earth System Model version 1.2. Over Scandinavia and Baffin Island, the respective locations in which the Scandinavian and Laurentide ice sheets are thought to have originated, low obliquity and perihelion at the boreal winter solstice are associated with lower ELA values, as would be expected from the orbital theory of the ice ages. Linear reconstructions of ELA variations over the past 800 kyr indicate that precession dominated ELA variations in Scandinavia and Baffin Island in the GFDL model, and in Scandinavia in the NCAR model. Obliquity and precession played equal roles in Baffin Island in the NCAR model. A decomposition of the ELA responses finds that the effects of ablation on ELA are much larger than the effects of precipitation. Overall, the findings of this study point to precession being a more important factor in glacial inception than obliquity, which contrasts with previous findings in which obliquity had a slightly larger effect on positive degree days (PDDs), a simple metric for ablation. This is likely due to differences in seasonality of melt from the ELA model and PDDs.

**Plain Language Summary** Large ice sheets alternately grew and decayed over Eurasia and North America during the past several million years. These cycles of glaciation are understood to be a response to changes in the shape of Earth's orbit, the timing of its closest passage to the Sun, and the tilt of its axis, which occur in predictable cycles. Using two global climate models and a model of how mass and energy are exchanged between a glacier and its environment, we found that the climate is more conducive to sea ice growth when the tilt of Earth's axis is smaller than today. The climate is also more conducive for growth when Earth is closest to the Sun in Northern Hemisphere winter rather than summer. Our results indicate that changes in orbital shape and timing of Earth's closest passage to the Sun exert a stronger effect than changes to the tilt of Earth's axis. We also found that changes in the processes that cause an ice sheet to lose mass (primarily melting) are more important than processes that cause it to gain mass (i.e., precipitation).

## 1. Introduction

Variations in Earth's obliquity (the tilt of Earth's axis), precession (the timing of when the Earth is closest to the Sun), and eccentricity (the shape of Earth's orbit) drive cyclical changes in the distribution of insolation causing Earth to experience glacial cycles on a timescale of 100 thousand years (ky). Obliquity, precession, and eccentricity are known as Milankovitch cycles (Milankovitch, 1998) and vary with timescales of 41 thousand years (ky), 19 and 23 ky, and 100 and 413 ky, respectively (Hays et al., 1976; Imbrie et al., 1984). Although it is known that these three orbital parameters drive climate variations, their relative effects are not fully understood and the main driver of the glacial cycle remains disputable. Ice volume proxy records of the early Pleistocene (2.588–0.781 Ma) are dominated by the 41 ky obliquity signal (Raymo & Nisancioglu, 2003). However, the late Pleistocene is dominated by 100 ky glacial cycles and it is unclear what marked this transition (Pisias & Moore, 1981; Ruddiman et al., 1989).

Precession affects the climate by changing the timing of perihelion; that is, the point in Earth's orbit at which it is closest to the Sun. Its effect on incoming solar radiation is felt at all latitudes in a given calendar month, although in opposite seasons in the two hemispheres. In climate model simulations, precession has been found to influence

northern high latitude climate through the sea ice albedo feedback and intensifies the increased meridional sea surface temperature gradient and moisture convergence (Jackson & Broccoli, 2003; Khodri et al., 2005).

Changes in obliquity produce smaller changes in instantaneous insolation than precession. Unlike precession, changes in obliquity cause variations in annual mean insolation. For example, lower obliquity leads to decreased annual mean insolation at high latitudes with a corresponding increase in low latitudes. Thus, a decrease in obliquity strengthens the meridional insolation gradient, which has the potential to strengthen atmospheric and oceanic circulation. Previous studies have found that lower obliquity increases poleward heat and vapor transport (Mantsis et al., 2011; Raymo & Nisancioglu, 2003), ocean to land vapor transport (Lee & Poulson, 2008), and poleward vapor transport through mid-latitude eddy activity (Mantsis et al., 2014). The clouds, water vapor, lapse rate, and surface albedo feedbacks further enhance these effects (Mantsis et al., 2011) and some feedbacks enhance the effect of obliquity on ice volume relative to precession (Tabor et al., 2014).

The relative importance of precession and obliquity in driving the glacial cycle has received considerable attention. It has often been assumed that June top-of-atmosphere insolation at 65°N drives glacial cycles, which is dominated by precession, and it has been proposed that the 100 ky glacial cycle is paced by every four or five precession cycles (Maslin & Ridgwell, 2005). There is evidence that precession was the dominant driver in the last glacial inception (Crucifix & Loutre, 2002) and that terminations were linked to precession driven ablation events (Barker et al., 2022). However, it has been postulated that the timing of the 100 ky glacial cycles could be attributed to terminations occurring every second or third obliquity cycle at times of high obliquity (Huybers & Wunsch, 2005; Ridgwell et al., 1999). It has been shown, through radiometric dating, that terminations were more likely to occur as a result of obliquity than as a result of precession, and obliquity played the major role in determining the rate at which climate approached interglacial conditions once terminated (Bajo et al., 2020).

Efforts have been made to quantify changes in glacial extent resulting from variations in Earth's orbit. This requires assumptions to be made about what metrics are good indicators to test the relative importance of obliquity and precession on climate, and how glaciers respond to the resulting changes in climate variables. One method is to assume variations in glacial extent are driven by some measure of insolation such as summer caloric half-year insolation at high latitudes, annual mean insolation (Loutre et al., 2004), insolation intensity integrated over the summer (Huybers, 2006; Huybers & Tziperman, 2008), or the meridional gradient of summer half-year insolation (Raymo & Nisancioglu, 2003). These yield varying results about the importance of obliquity versus precession on the glacial cycle, demonstrating the sensitivity of results to which measure of summer insolation is chosen. Another method is to assume ablation is proportional to summertime temperature. Positive degree-days (PDDs), which sum the mean daily temperature for days above 0°C, can be used as a proxy for ablation (Braithwaite, 1995; Jackson & Broccoli, 2003; O'Neill & Broccoli, 2021). However, PDDs neglect important climate variables that can influence ablation, such as insolation, wind, albedo, and cloudiness. PDDs also do not account for sublimation, which can occur in cold, dry places most suitable for glaciation. A better approach to estimating the response of a glacier to changes in climate is to use an energy balance method which includes all relevant climate variables and sublimation (Kayastha et al., 1999). A common assumption in focusing on metrics based on insolation or temperature, such as those described above, is that variations in glacial extent are primarily driven by ablation. Although this may be true, a more comprehensive approach would also include the effects of changes in accumulation, which have also been proposed to play an important role in glacial-interglacial variations (Gildor & Tziperman, 2001).

Our earlier analysis (O'Neill & Broccoli, 2021) examined the influences of obliquity and precession on ablation and accumulation but could not quantify the combined effects on glacial mass balance. This shortcoming is addressed in this study by implementing the surface energy and mass balance (SEMB) model developed by Rupper and Roe (2008) to calculate the equilibrium-line altitude (ELA), the height on a glacier where accumulation and ablation are in balance annually. As in O'Neill and Broccoli (2021), climate forcing for the SEMB model is obtained from idealized, single-forcing atmosphere-ocean general circulation model (AOGCM) simulations. We examine the responses of ELA to changes in obliquity and precession, with particular focus on Scandinavia and Baffin Island, the proposed locations of the inception of the Scandinavian and Laurentide ice sheets respectively (e.g., Dong & Valdes, 1995). In addition to the implementation of the SEMB model, we further extend the analysis of O'Neill and Broccoli (2021) by using climate forcing from two different AOGCMs.

**Table 1**
*Obliquity, Longitude of Perihelion, and Eccentricity Values of the Simulations Run for GFDL CM2.1 and NCAR CESM*

|  | Obliquity (°) | Longitude of perihelion (°) | Eccentricity |
|---|---|---|---|
| Preindustrial | 23.439 | 102.93 | 0.0167 |
| Low obliquity | 22.079 | Preindustrial | Preindustrial |
| High obliquity | 24.480 | " " | " " |
| AE perihelion | Preindustrial | 0 | 0.0493 |
| WS perihelion | " " | 90 | 0.0493 |
| VE perihelion | " " | 180 | 0.0493 |
| SS perihelion | " " | 270 | 0.0493 |
| Zero eccentricity | " " | – | 0 |

## 2. Methods

### 2.1. Atmosphere-Ocean General Circulation Models

The SEMB model was driven by output from experiments run on two AOGCMs, the Geophysical Fluid Dynamics Laboratory (GFDL) Climate Model 2.1 (CM2.1) (Delworth et al., 2006; Erb et al., 2015) and the National Center for Atmospheric Research (NCAR) Community Earth System Model (CESM) version 1.2 (Erb, Jackson, Broccoli, et al., 2018; Hurrell et al., 2013). The experiments are idealized single-forcing simulations designed to quantify the effects of variations in a single orbital forcing in isolation, keeping all else set to preindustrial (i.e., 1860) values. The simulations, which used the same forcing for each model, comprised of two obliquity experiments where obliquity was set to the high and low extremes of the past 600 ky (Berger & Loutre, 1991), four precession experiments where the date of perihelion was set to the northern hemisphere (NH) autumnal equinox (AE), winter solstice (WS), vernal equinox (VE), and summer solstice (SS) with eccentricity set to the maximum of the past 600 ky, a zero-eccentricity experiment, and a preindustrial experiment where all forcings were set to preindustrial values (Table 1). Each simulation was run for 500 years to approach a quasi-equilibrium surface climate, defined as the point where systematic trends in large-scale surface climate are minimal, with the following 100 years used for analysis.

To ensure all experiments are on a consistent calendar, and since Earth's orbital speed is dependent on its distance from the sun, a calendar adjustment was applied to the precession experiments such that a month is defined by a 30° arc of Earth's orbit (Pollard & Reusch, 2002). Atmospheric composition, ice sheets, and sea level were set to preindustrial values and the model output is therefore applicable to an interglacial climate. Consequently, the results from these model simulations are most relevant to glaciation, not deglaciation, since running the simulations with glacial atmospheric composition and ice sheets would likely yield different results.

The calendar-adjusted response of top-of-atmosphere (TOA) insolation to precession and changes in obliquity is shown in Figure 1, in which the left panel displays the difference between the low and high obliquity experiments and the right panel the difference between the WS and SS experiments. Because the calendar adjustment essentially changes the lengths of the months to account for Earth's varying orbital speed but the plotting software assumes that the months have the same lengths in both experiments, the visual appearance of the seasonal insolation pattern at higher latitudes in the right panel of Figure 1 is distorted. This distortion is non-negligible, but not as drastic as it would be if the calendar adjustment had not been made. For both cases, insolation is substantially reduced during a period centered on the boreal summer solstice. The effects of precession are larger, due in part to the large eccentricity used in the precession experiments, and have a sharper maximum in magnitude. Although glaciers and ice sheets would be expected to be most sensitive to surface rather than TOA forcing, the
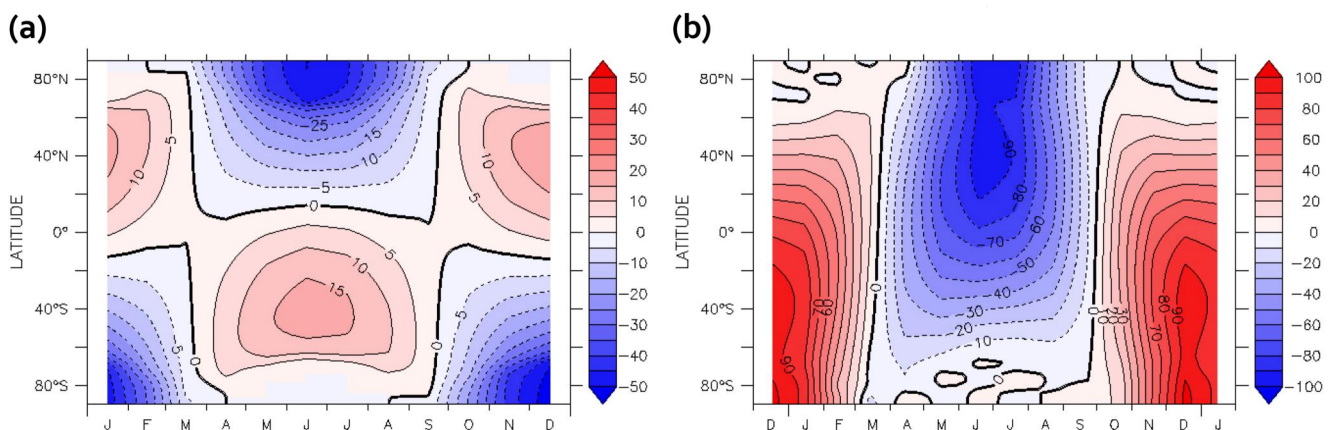


**Figure 1.** Seasonal changes in zonal-mean insolation (W m$^{-2}$) for the (a) Low–High obliquity and (b) WS–SS experiments as a function of latitude.

downward solar radiation at the surface largely follows the pattern of TOA forcing, albeit with smaller magnitude because of cloud feedbacks that partially offset the direct forcing, as noted by Erb et al. (2013).

## 2.2. Mass Balance Model

We used the SEMB model developed by Rupper and Roe (2008) to calculate the ELAs from our modeled climate variables. The model is forced by air temperature, relative humidity, wind speed, pressure, incident shortwave radiation, atmospheric emissivity, lapse rate, and precipitation, to calculate the height at which accumulation and ablation are in balance annually for a hypothetical ice sheet. Accumulation is greater than ablation above the ELA (the accumulation zone) and ablation is greater than accumulation below the ELA (the ablation zone). Changes in the ELA can be used to understand the relationship between climate and glaciation potential. A decrease in the ELA makes it easier for a glacier to form, and thus a forcing that decreases the ELA makes conditions more favorable for glaciation.

The ELA model is composed of nested surface energy balance and mass balance algorithms such that the elevation where both balances are satisfied is the ELA. Equation 1 is the surface energy balance equation and Equation 2 is the mass balance equation.

$$Q_m = \text{SW} + \text{LW} + Q_s + Q_l + Q_g \tag{1}$$

$$\text{Monthly Accumulation} = \text{melting} + \text{evaporation} + \text{sublimation} \tag{2}$$

In the surface energy balance equation, $Q_m$ is the energy available for melting each month, SW is the shortwave radiation flux absorbed by the surface, LW is the net longwave radiation flux, $Q_s$ is the sensible heat flux, $Q_l$ is the latent heat flux, and $Q_g$ is the heat conduction from the subsurface, which is small enough that it is assumed to be zero. The ELA model uses these equations to find the temperature at which annual ablation equals annual accumulation and the climatological lapse rate is used to find the height at which this temperature occurs (i.e., the ELA). We calculated the ELAs over every grid point for each of the GFDL and NCAR experiments, and our output included the ELAs and the annual melt, evaporation, and sublimation totals.

The ELA model was run as described by Rupper and Roe (2008), except that the climate information used to drive the model was taken from the GFDL and NCAR orbital simulations instead of from modern reanalysis. Climatological monthly mean model output was used to determine input quantities, including downward shortwave radiation, precipitation, lapse rate, wind speed, and humidity. The ELA model assumes that all precipitation falls as snow.

## 2.3. Linearly Reconstructed Time Series

A goal of this study was to compare the effects of obliquity and precession on the ELA. More specifically, we would like to know whether variations in obliquity or precession make the larger contribution to ELA variations during the late Pleistocene. To reconstruct how variations in obliquity and precession over the past 800 ky would combine to affect the potential for glaciation, we used the method of Erb et al. (2015) to approximate how our ELA variable would have responded to past changes in orbital forcings. This method assumes that the effects of obliquity changes are proportional to the magnitude of the change, the effects of precession are proportional to orbital eccentricity, and the effects of obliquity and precession can be linearly summed. Equations 3–5 are the linear reconstruction equations developed by Erb et al. (2015). X is a climatic variable (in this case, ELA) from the experiment indicated by its subscript, and $\Delta$X is the anomaly of that variable (relative to the preindustrial simulation) resulting from the forcing indicated by its subscript. The constants $\epsilon$, $e$, and $\omega$ represent obliquity, eccentricity, and longitude of perihelion (in degrees), respectively, with subscripts indicating values taken from the corresponding experiment. Equation 3 is the obliquity component time series where X is forced only by obliquity, and Equation 4 is the precession component time series where X is forced only by eccentricity-modulated precession. Equations 3 and 4 are summed in Equation 5 to create the time series of the variable forced by all orbital forcings. These equations can be used to reconstruct $\Delta X$ for any combination of $\epsilon$, $e$, and $\omega$.

$$\Delta X_{\text{obliq}} = \frac{\epsilon - \epsilon_{\text{preind}}}{\epsilon_{\text{high}} - \epsilon_{\text{low}}}(X_{\text{high}} - X_{\text{low}}), \tag{3}$$

$$\Delta X_{\text{prec}} = \frac{e}{e_{\text{prec}}}\left[\frac{X_{\text{AE}} - X_{\text{VE}}}{2}cos\,(\omega) + \frac{X_{\text{WS}} - X_{\text{SS}}}{2}sin\,(\omega) + \left(\frac{X_{\text{AE}} + X_{\text{WS}} + X_{\text{VE}} + X_{\text{SS}}}{4}\right) - X_{0ecc}\right], \quad (4)$$

$$\Delta X_{\text{orbit}} = \Delta X_{\text{obliq}} + \Delta X_{\text{prec}}, \quad (5)$$

Actual values of obliquity, eccentricity, and longitude of perihelion for the past 800 ky (Berger & Loutre, 1999) are introduced in these equations to reconstruct time series of ELA over that period. We reconstructed time series at every point north of 45°N for GFDL and NCAR ELAs. We calculated both the obliquity component (Equation 3) and precession component (Equation 4) time series, which sum to the full orbitally forced time series (Equation 5).

Erb et al. (2015) compared reconstructed climate states based on this method with the results of "snapshot" paleoclimate simulations in which multiple forcings were applied simultaneously. They found this linear reconstruction method to be quite successful at reproducing large-scale patterns of temperature and precipitation in mid-Holocene and last glacial maximum simulations. They also found some variables, such as the Atlantic meridional circulation and sea ice extent, in which the agreement between the reconstructions and the snapshot simulations was not as good. When interpreting the results, one should keep in mind that the linear reconstructions are only approximations of how a coupled climate model would respond if forced continuously with the actual variations in orbital parameters.

Note that the reconstructed ELA time series should not be interpreted as an attempt to model the history of ELA variations. Because the GFDL and NCAR experiments simulate responses to orbital forcing relative to an interglacial base climate state, the ELA reconstructions are a sensitivity experiment. They do not include the effects of changes in atmospheric composition and ice sheet dynamics, which profoundly affected past variations in climate.

## 3. Results

### 3.1. ELA

Figures 2 and 3 show the differences between each of the obliquity and precession experiment ELAs and the preindustrial experiment ELAs. As expected, the low obliquity experiments had lower ELAs than the high obliquity experiments since a decrease in obliquity causes a cooling in annually averaged temperatures in this region, making conditions more favorable for glaciation. Among the precession experiments, the WS simulations had the largest reduction in ELA and the SS simulations had the largest increase in ELA, consistent with the orbital theory of the ice ages. The ELA anomalies in the VE and AE precession experiments were smaller. In comparing the GFDL and NCAR models, the overall patterns of response were similar, but the NCAR model produces larger anomalies in some polar regions. This difference in the magnitude of the ELA response will be discussed in a subsequent section.

### 3.2. Time Series Analysis

Figure 4 shows the ranges (i.e., the difference between the extremes) of the obliquity and precession component ELA time series over the north polar region. Because the values of obliquity in the obliquity experiments and the value of eccentricity in the precession experiments are set to the extremes of the past 600 ky, the ranges of the reconstructed component time series represent the maximum effect each orbital parameter can have on the ELA.

The range of the obliquity time series is simply the low obliquity experiment minus the high obliquity experiment, which represents the difference in ELA between the most glaciation-favorable and least glaciation-favorable scenarios. The calculation of the range of the precession time series is more complicated because the perihelion date that minimizes the ELA (and is therefore more conducive for glaciation) can be different at every point. We calculated the range of the precession time series by finding the dates of perihelion that minimized and maximized the ELA at each point and subtracted the maximum from the minimum. Defined in this way, the range is expressed as the difference in ELA between the perihelion dates that are most and least favorable for glaciation. Note that ranges at each point are calculated independently, thus allowing the perihelion dates that maximized and minimized the ELA to vary with location. However, we found that in both models, almost all locations in this region had minimum ELA when the perihelion date was close to the winter solstice, which is consistent with the
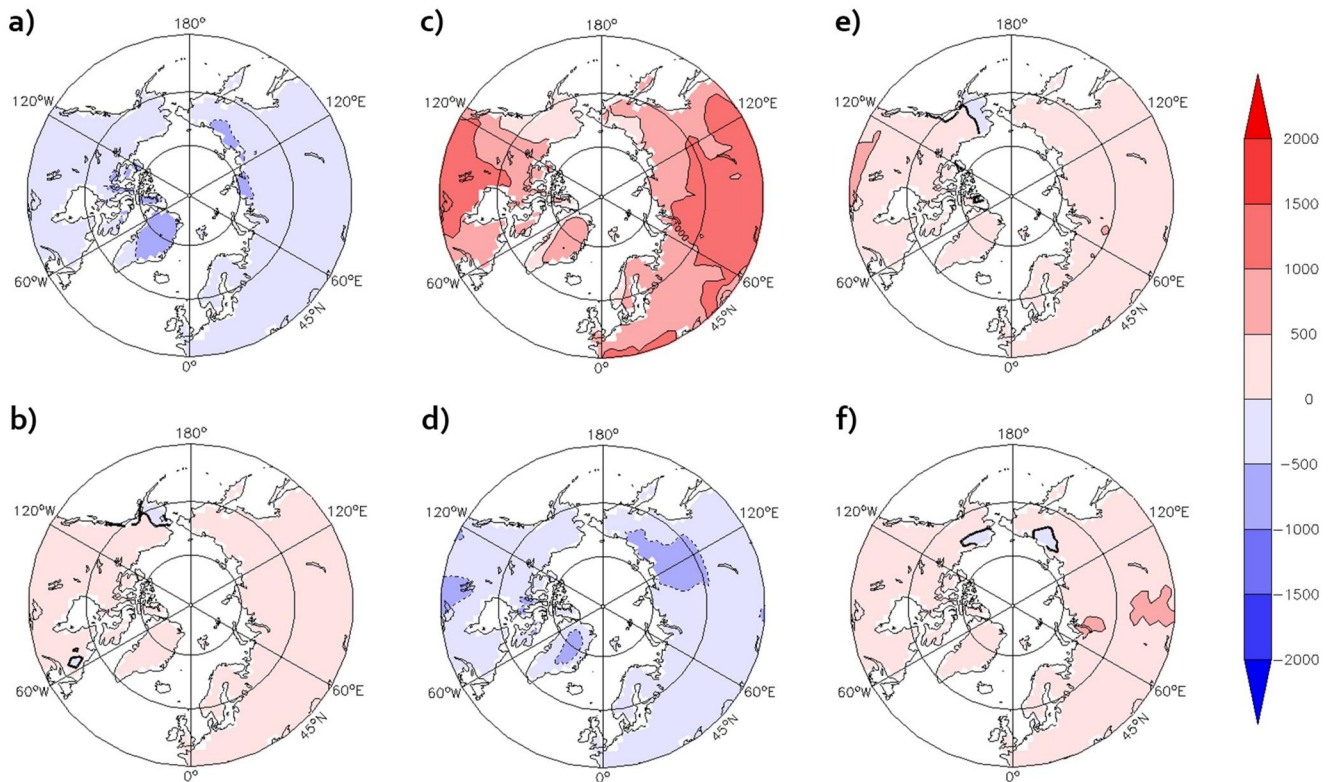
**Figure 2.** Geophysical Fluid Dynamics Laboratory experiment equilibrium line altitude anomalies relative to the preindustrial experiment (in meters) for (a) low obliquity, (b) high obliquity, (c) summer solstice perihelion, (d) winter solstice perihelion, (e) vernal equinox perihelion, and (f) autumnal equinox perihelion.

Milankovitch hypothesis. Precession had a greater effect on the ELA in continental interiors, indicated by their larger ranges there. Additionally, the NCAR experiments exhibited greater magnitudes north of about 65°N, particularly in the islands of the Canadian Arctic.

To investigate the relative importance of obliquity and precession to ELA variations in locations where the Scandinavian and Laurentide ice sheets were initiated, we calculated regional ELA time series for Scandinavia and Baffin Island using ELA values averaged over each region. We summed the obliquity and precession component time series to create time series that combined the effects of variations in obliquity and precession. From these regional time series, we determined the percent variance that was contributed by variations in obliquity and precession (Figure 5), thereby estimating the relative importance of obliquity and precession to the changes in the ELA. (Note that the percentage of the variance resulting from variations in obliquity and precession must sum to 100% by construction.)

In Scandinavia, obliquity was responsible for 28% of the ELA variance in the GFDL model and 31% of the ELA variance in the NCAR model. In Baffin Island, there was a larger difference between the two models, with obliquity responsible for 29% of the variance in the GFDL model and 51% in the NCAR model. Overall, the contribution from precession is greater than or equal to that of obliquity. This finding is in contrast with the results from O'Neill and Broccoli (2021). In that study using only GFDL model output and using PDDs as a metric of ablation, obliquity was found to be responsible for 58% and 61% of the PDD variance in Scandinavia and Baffin Island, respectively. Thus, precession is having a larger effect on the ELA than it was found to have on PDDs, implying precession could be playing a larger role in glaciation than our previous study suggested. Possible reasons for this difference will be discussed in Section 4.

### 3.3. Contributions of Ablation and Accumulation to the ELA

The Rupper and Roe (2008) model uses climate variables from the AOGCM experiments to calculate the ELA. Air temperature, relative humidity, wind speed, pressure, incident shortwave radiation, atmospheric emissivity,
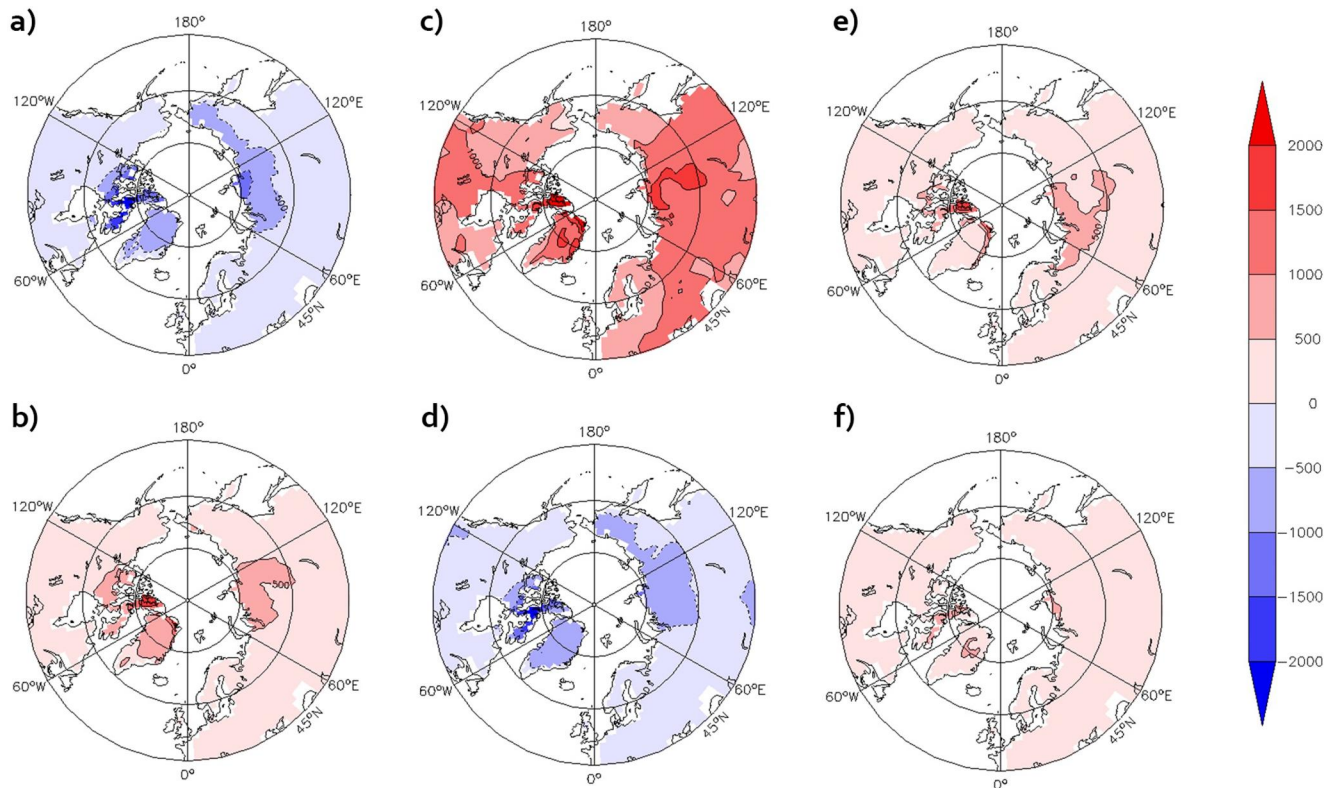
**Figure 3.** Same as Figure 2 but for National Center for Atmospheric Research.

and lapse rate are used to calculate ablation and precipitation is used for accumulation. To examine the individual contributions of accumulation and ablation, we conducted ELA simulations in which only ablation-related or only precipitation-related variables were used as input to the model. For example, a precipitation-only low obliquity simulation would use as input the precipitation from the low obliquity experiment and all other climate variables from the high obliquity experiment, and the precipitation-only high obliquity simulation would use the opposite combination. A parallel approach was used for ablation-only simulations. For each of the precession experiments, an ablation-only ELA simulation, for example, would use the ablation-related variables from the corresponding precession climate model experiment and precipitation from the zero-eccentricity experiment. To isolate the effects of cloud cover, humidity, wind speed, and the direct effects of insolation, we conducted additional ELA simulations that allowed only temperature and precipitation to change.

Using the linear reconstruction Equations 3–5, we then calculated the time series for the effects of obliquity and precession on the ELA for the ablation-only, precipitation-only, and temperature-plus-precipitation-only cases. We will refer to the resulting ELA time series as the ablation-only ELA, the precipitation-only ELA, and the precipitation-plus-temperature-only (P + T-only) ELA. For comparison, we will refer to the ELA calculated from the combined effects of ablation-related and precipitation-related variables as the standard ELA. (Note that because of the inherent nonlinearity of the energy and mass balance model, the combined effect of changes in ablation and precipitation is not a linear sum of the ablation-only and precipitation-only time series.)

We compared the ranges of the ablation-only, precipitation-only, and P + T-only ELA time series, including the effects of both precession and obliquity variations, to the standard ELA time series (Figure 6). The standard ELA sensitivity is comparable for both models in Scandinavia, but the NCAR model has more than double the sensitivity of the GFDL model in Baffin Island, consistent with the greater sensitivity of the NCAR in that region discussed in reference to Figure 4. The ablation-only ELA ranges were approximately equal to those of the standard ELA and the precipitation-only ELA ranges were comparatively very small. The magnitude of the changes in the precipitation-only ELA time series were small enough compared to those of the ablation-only ELA time series to conclude that ablation was the dominant driver of ELA variations and that precipitation did not play
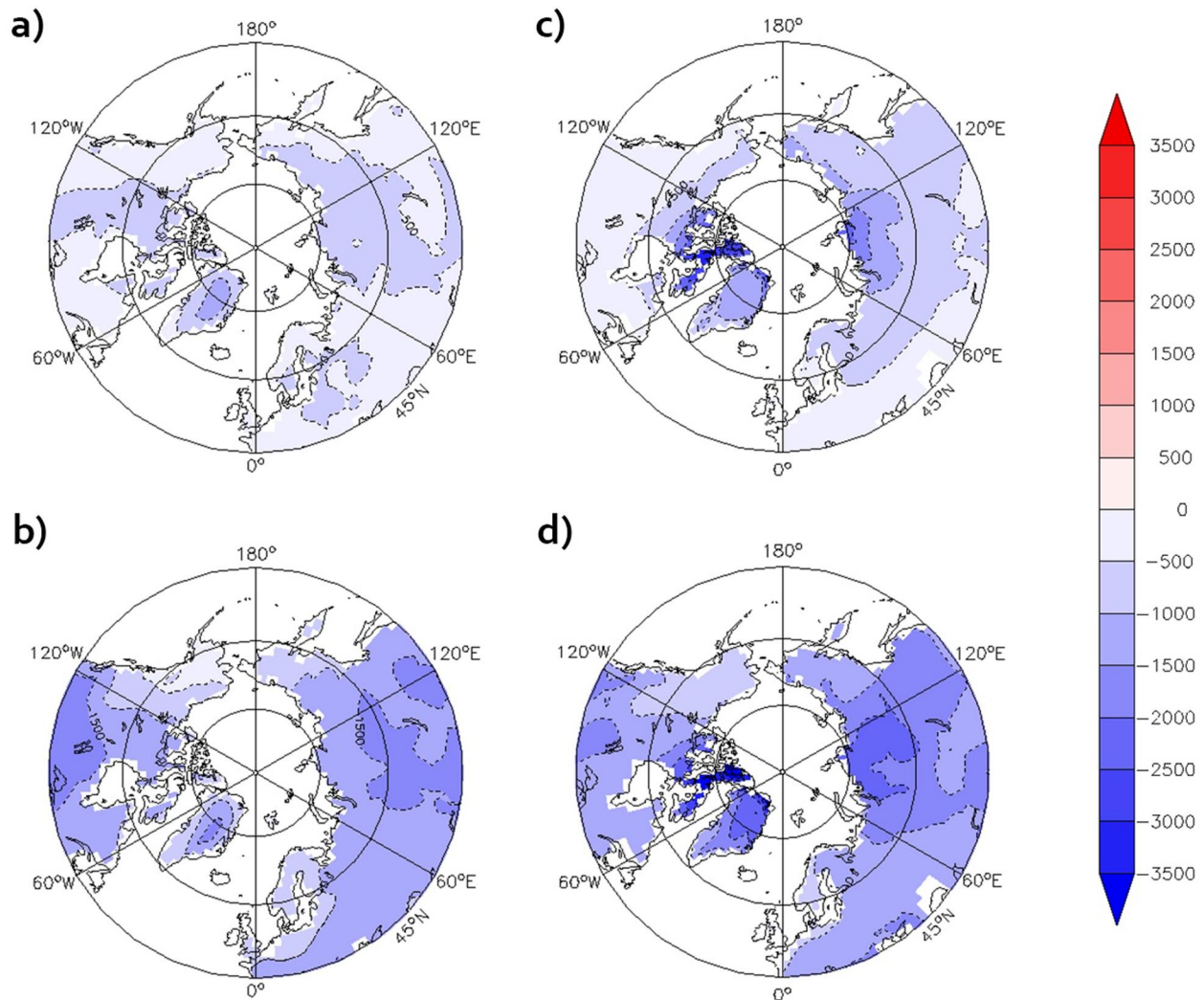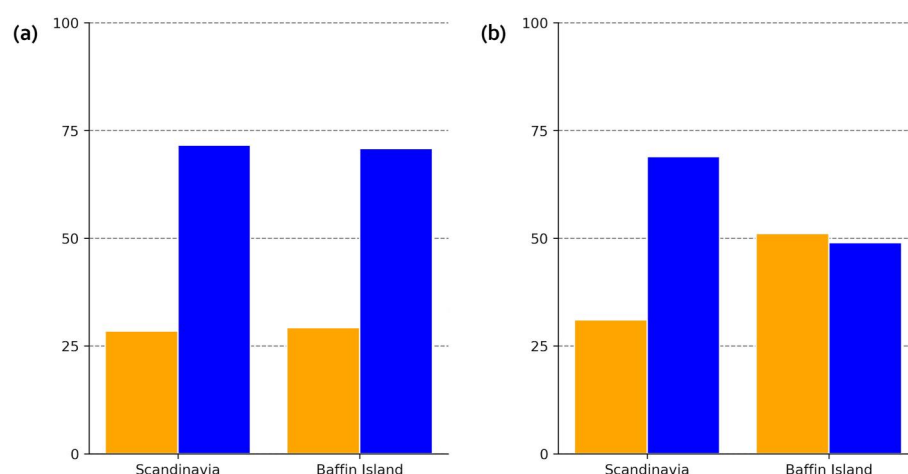
**Figure 4.** Ranges (in meters) of component equilibrium line altitude time series of (a) Geophysical Fluid Dynamics Laboratory (GFDL) obliquity, (b) GFDL precession, (c) National Center for Atmospheric Research (NCAR) obliquity, and (d) NCAR precession.

a large role. We also found that in both regions and for both GFDL and NCAR, the ablation-only ELA time series had variance contributions from obliquity and precession that were almost identical to those of the standard ELA time series (not pictured).

Comparison of the P + T-only ELA ranges with the standard ELA indicates that the ELA response is considerably smaller if only the effects of temperature on ablation are provided as forcing. Excluding the effects of cloud cover, humidity, wind speed, and the direct effects of insolation leads to a reduction of about 20%–50% in the range of ELA variations relative to the standard ELA, indicating that temperature is not the only influence on ablation. We will return to this finding in a subsequent section.

The contributions of changes in ablation and precipitation to the overall response of ELA to variations in obliquity and precession depend upon their phasing. For obliquity, we have depicted the range of the standard ELA response by subtracting the ELA from the low obliquity experiment from that of the high obliquity experiment. We have followed the same convention for the ablation-only (Figures 7a and 7b) and precipitation-only ELA responses (Figures 8a and 8b). For precession, we chose the same phasing that produced the most extreme standard ELA values (i.e., corresponding to the ranges depicted in Figures 4c and 4d) to determine the ablation-only (Figures 7c and 7d) and precipitation-only (Figures 8c and 8d) ELA responses.
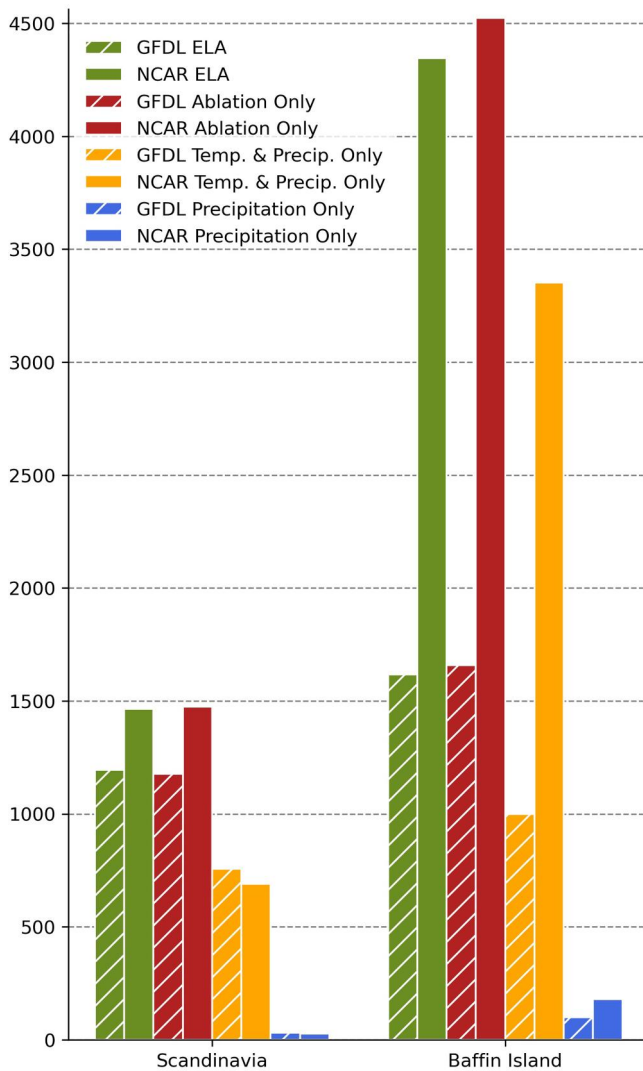
**Figure 5.** Percentage of variance in the equilibrium line altitude time series resulting from obliquity (orange) and precession (blue) in Scandinavia and Baffin Island for (a) Geophysical Fluid Dynamics Laboratory and (b) National Center for Atmospheric Research.

The ablation-only ELA maps (Figure 7) look very similar to the maps of the standard ELA's component time series ranges (Figure 4). In both models, the precession maps are all negative (Figures 7c and 7d), indicating that the ablation-only ELA is decreasing, making conditions more favorable for glaciation. The obliquity maps also have all negative values (Figures 7a and 7b), implying that a decrease in obliquity decreased the ablation-only ELA. These responses imply that when only ablation changes are used as climate forcing, ELA responds to variations in obliquity and precession in a manner very similar to the response of ELA to full climate forcing. This result is not surprising given that the majority of the ELA response was found to be provided by ablation (Figure 6).

The precipitation-only ELA maps have smaller magnitudes than the ablation-only ELA maps over most polar and subpolar regions (Figure 8). The obliquity effect has the opposite sign for precipitation-only ELAs on most of the maps; the predominance of red shades in many regions means that precipitation changes raise the ELA at those locations, making conditions less favorable for glaciation (Figures 8a and 8b). The likely cause of this response is that the low obliquity experiments have less precipitation than the high obliquity experiments because of a generally weaker hydrologic cycle in a colder climate. The precession maps (Figures 8c and 8d) include areas of ELA decrease (blue) and ELA increase (red), a pattern with more spatial variability than the precipitation-only responses to obliquity. In the areas where the precipitation-only ELA response is positive, the effect of precession on precipitation works against the glaciation-favorable effects of ablation, while in the regions of precipitation-only ELA decrease, the effects of both ablation and precipitation are reducing the ELA. The effects of precipitation-only ELA changes tend to be small over Baffin Island and Scandinavia, consistent with the small precipitation-only components in Figure 6. Other areas have larger responses. For example, Northeast Asia has positive ELA changes in all four precipitation-only maps likely because the colder summers in both the obliquity and precession scenarios reduced summer precipitation, and warmer winters in the precession scenario did not result in much of an increase in wintertime precipitation because of the low winter temperatures there and the nonlinearity of the Clausius-Clapeyron equation.

### 3.4. Prominence of Melt and Sublimation in Ablation

The ELA model determines the ablation required to balance the precipitation at the ELA as the sum of melting, sublimation, and evaporation that would occur at that altitude. For both GFDL and NCAR, the ablation was predominantly in the form of melt, with increased sublimation where model temperature and precipitation were small annually (Figures 9 and 10). There is a clear relationship between precipitation and melt and precipitation and sublimation. Increased precipitation is associated with an increase in melt and a decrease in sublimation. Temperature has a similar relationship, with the importance of melt generally increasing with increasing temperature, except for some points that have smaller melt fractions (and larger sublimation) despite having high temperatures. These points, which trail downward from the main cluster of points in Figures 9b and 10b, have

**Figure 6.** Ranges (in meters) of standard (green), ablation-only (red), precipitation-plus-temperature-only (orange), and precipitation-only (blue) equilibrium line altitude time series from Geophysical Fluid Dynamics Laboratory (striped) and National Center for Atmospheric Research (solid) models.

relatively low annual precipitation rates, as shown in Figures 9c and 10c, where only points with rates below 0.45 m/yr are plotted. At these locations, the precipitation is low enough that losses from sublimation are sufficient to achieve mass balance.

Scandinavia and Baffin Island are plotted on Figures 9 and 10 as "S" and "B," respectively. At both locations, melt is the dominant form of ablation, but with a notable difference. Scandinavia lies at a lower latitude than Baffin Island with the North Atlantic Ocean upstream. This results in Scandinavia being warmer and having greater precipitation rates than Baffin Island. As a result, Baffin Island, although still dominated by melt, had higher rates of sublimation and lower rates of melt than Scandinavia.
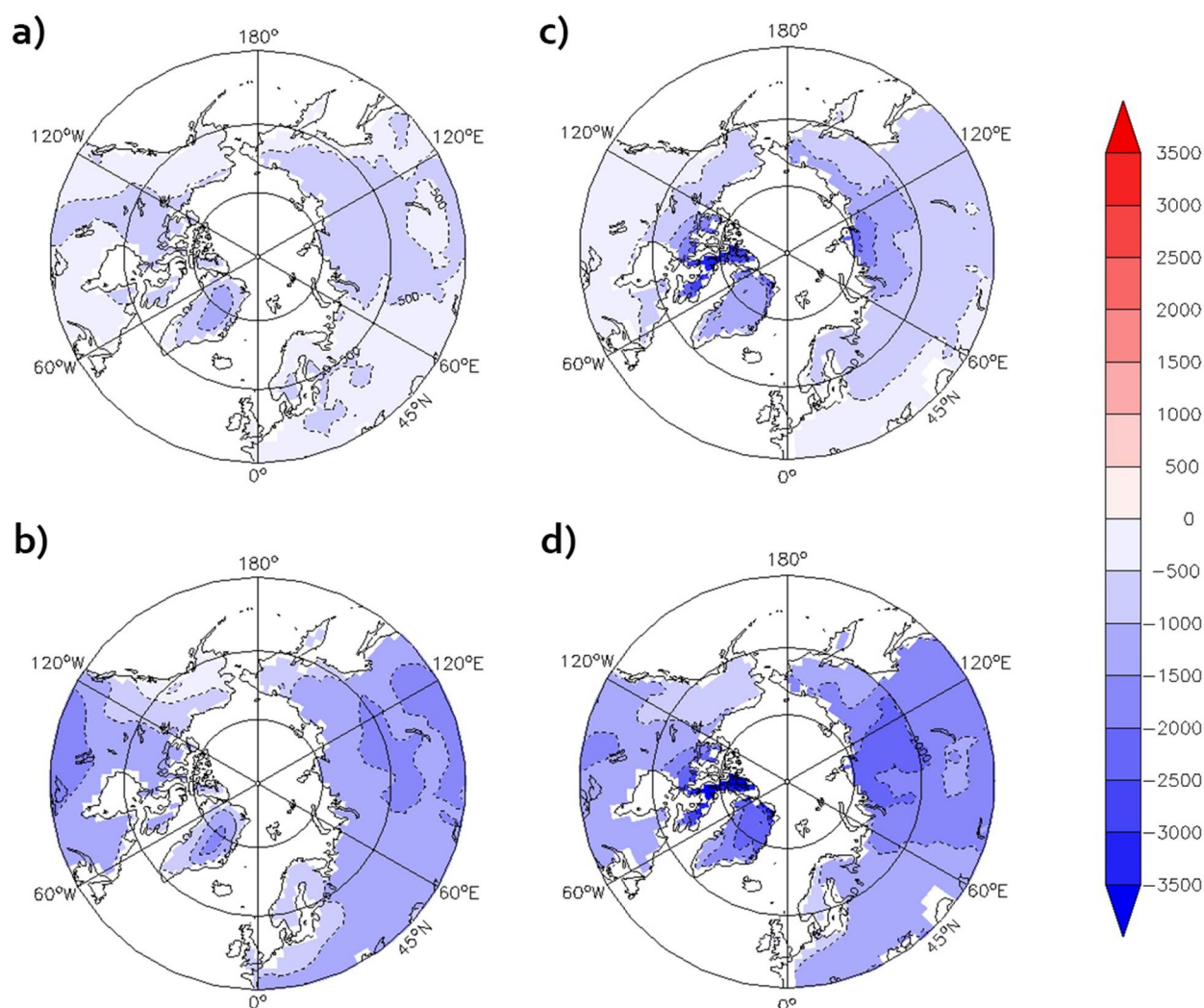
## 4. Discussion

### 4.1. Comparison of Scandinavia and Baffin Island in GFDL and NCAR

We used model output from the GFDL CM2.1 and the NCAR CESM to determine how sensitive the results are to the model chosen. We found similar results, but with key differences in the polar region. The NCAR experiments had greater ELA anomalies north of about 65°N, especially in the Canadian Arctic islands, compared to GFDL (Figure 4). This can be attributed to differences in the baseline climate state in this region. Polar temperatures in the NCAR model are colder than in GFDL (Figure 11). Summer temperatures are specifically colder in northern Canada, Greenland, and northernmost Eurasia.

A colder baseline climate supports more extensive sea ice and snow cover, allowing albedo feedbacks to play a larger role. This is particularly important in summer, when high latitude surface air temperatures are not too far from the freezing point. As a result, changes in ELA caused by changes in orbital parameters are magnified in NCAR's polar region. Baffin Island is part of this cooler region, resulting in ELA anomalies that are more than twice as large as those of GFDL (Figure 6). Differences in temperature between GFDL and NCAR over Scandinavia are not as large and vary with season, resulting in similar ELA anomalies (Figure 6). Thus, the magnitude of the effects of obliquity and precession on the ELA are sensitive to how the AOGCM models temperature.

In NCAR, obliquity and precession contributed nearly equally to variations in Baffin Island ELAs (Figure 5). This poses the question as to why Baffin Island in NCAR was the one scenario with a strong obliquity contribution. As discussed, the Arctic region in NCAR is colder than in GFDL. This means NCAR has a stronger summertime meridional temperature gradient and more extreme temperatures annually. Obliquity dominates the meridional gradient of temperature and variations in annual temperature since the insolation forcing associated with precession changes sign during the annual cycle, leading to only small variations in temperature annually. It can be postulated that the more significant role temperature played in Baffin Island in NCAR amplified the effects of obliquity relative to GFDL.

### 4.2. ELA Versus PDD Method

Another goal of this work was to build upon our previous analyses in which we explored the effects of changes in obliquity and eccentricity-modulated precession using PDDs as a proxy for ablation (O'Neill & Broccoli, 2021). PDDs represent the cumulative sum of mean daily temperatures above 0°C, thus only considering ablation a function of temperature. Based on output from the same GFDL simulation examined here, we found that obliquity was responsible for 58% of the variance in annual PDDs in Scandinavia, and for 61% in Baffin Island, suggesting that obliquity was a slightly more important driver of ablation than precession in these regions. In contrast, the

**Figure 7.** Map of ranges of ablation-only time series (in meters) for (a) Geophysical Fluid Dynamics Laboratory (GFDL) obliquity, (b) GFDL precession, (c) National Center for Atmospheric Research (NCAR) obliquity, and (d) NCAR precession, at the precession phasing that maximizes the effect of precession on the equilibrium line altitude.

analysis in the current study based on the GFDL model indicated that precession is the dominant driver, with obliquity responsible for only 28% of the ELA variance in Scandinavia and 29% in Baffin Island.

The PDD method is a simplified representation of ablation that assumes that ablation is a function of only temperature, implicitly assuming that mass loss primarily comes from melt. Sublimation is not considered. Although O'Neill and Broccoli (2021) also considered orbital effects on accumulation, there was no quantitative basis for comparing its contribution with that of ablation. The ELA method used in the current study incorporates the effects of sublimation, which is likely to occur in our cold, dry polar regions of interest. Additionally, the ELA is determined from both energy and mass balances, so it integrates the role of precipitation which could not be quantitatively combined with PDDs. While PDDs and ELAs cannot be directly compared due to the higher complexity of ELAs and incorporation of a mass balance model, there is interest in comparing how a more complex metric compares to the simple PDD method.

After considering the differences between the PDD method used by O'Neill and Broccoli (2021) and the ELA modeling conducted in the current study, it is reasonable to conclude that the greater importance of precession in the latter originates from the use of a more physically based approach. The analyses described in Section 3 allow us to engage in informed speculation about a specific cause of the difference. The ablation-only and precipitation-only ELA model simulations indicate that the inability to account for precipitation in the PDD method is not a
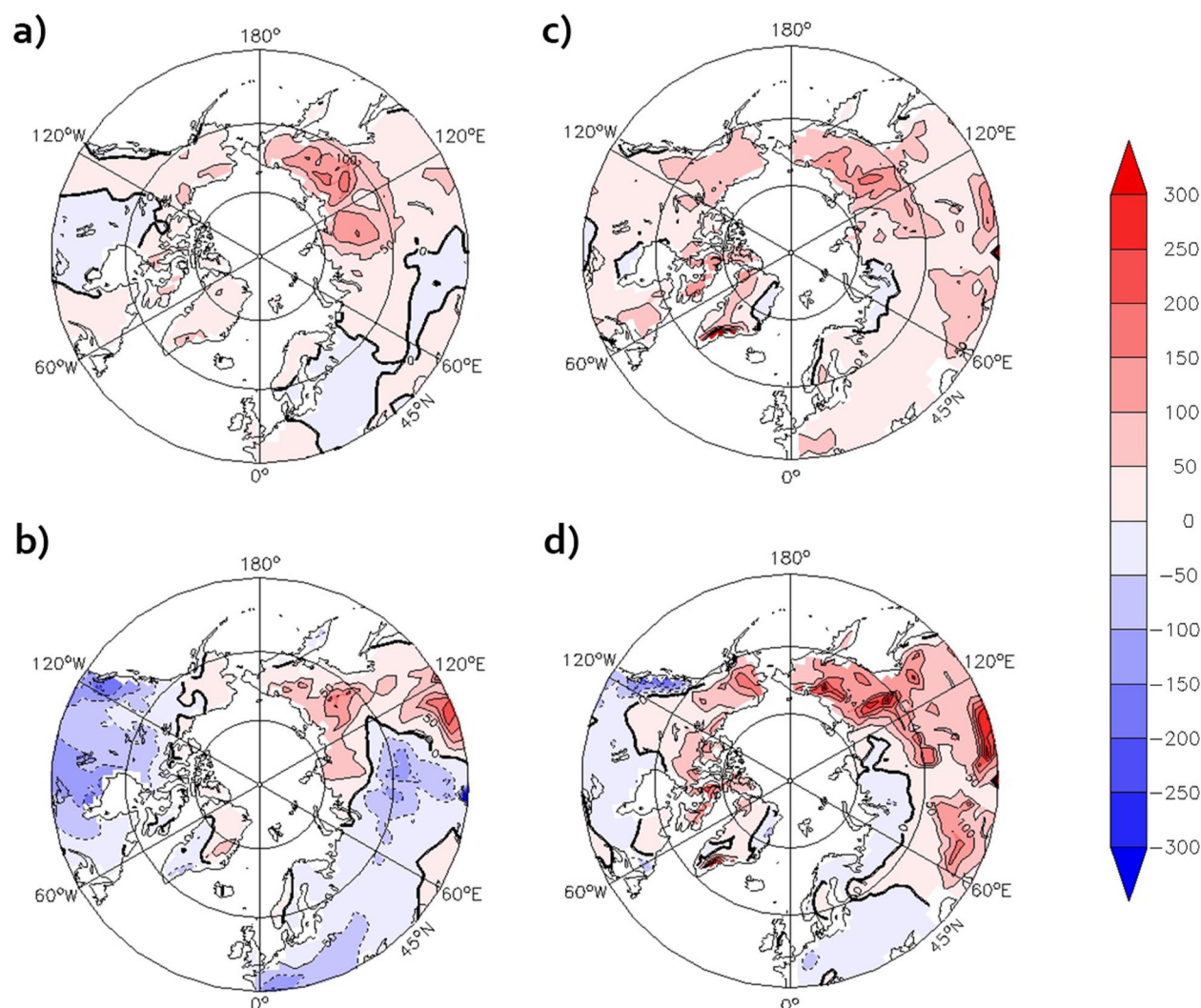
**Figure 8.** Same as Figure 7 but for precipitation-only time series.

likely cause, as precipitation makes a negligible contribution to simulated ELA variations. The neglect of sublimation can also be effectively ruled out, as Figures 9 and 10 show that ablation was dominated by melt in Scandinavia and Baffin Island.

A more likely explanation is an important difference in the seasonality of ablation between the PDD and ELA methods (Figure 12). PDDs are greatest in midsummer, but the peak is broad and nonzero PDDs occur in the transition seasons, especially in Scandinavia. In the ELA model, the majority of melt came from July in each experiment, with zero melt in any month before April or after September. The P + T-only ELA model simulations discussed in Section 3.2 also indicate that variables not directly related to temperature, such as insolation, humidity, and wind speed, contribute substantially to the standard ELA response. With a sharper peak closer to the summer solstice, ablation in the ELA model is more sensitive to precession, which produces larger insolation anomalies than obliquity variations, but with the anomalies confined to the half-year centered on the perihelion date. In contrast, obliquity variations can affect annual mean insolation, thus impacting temperature (and PDDs) throughout the year.

## 5. Conclusions

In this study, we used a SEMB model (Rupper & Roe, 2008) to calculate ELAs using climate forcing from two AOGCMs. The ELAs were calculated for eight idealized single-forcing simulations which represent eight orbital
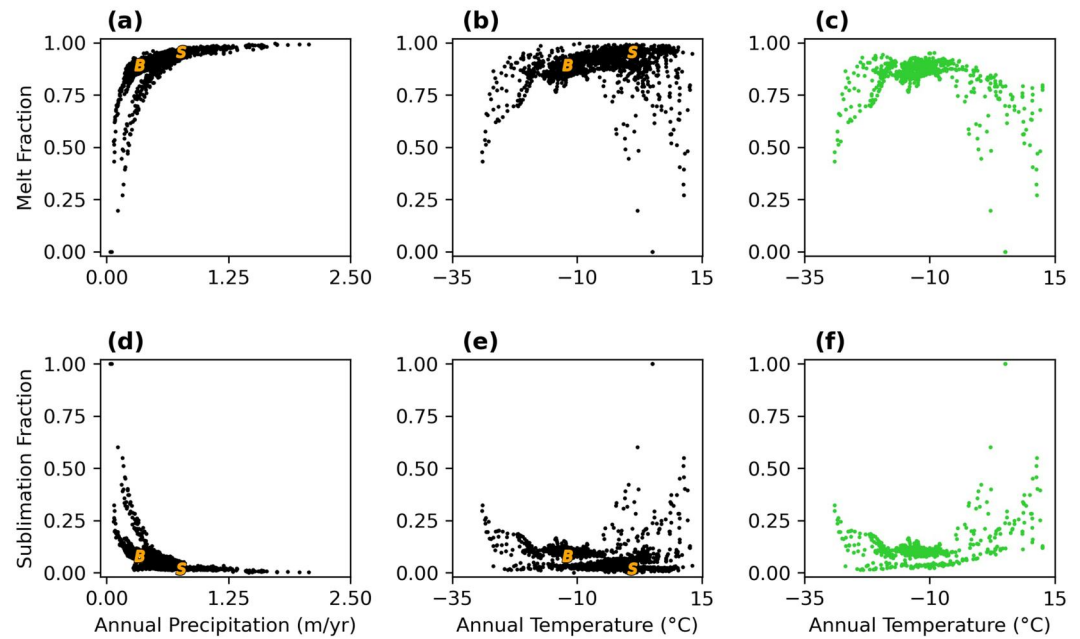
**Figure 9.** Scatter plots of all Geophysical Fluid Dynamics Laboratory land points north of 45°N in the preindustrial experiment comparing (a) annual precipitation and melt fraction, (b) annual temperature and melt fraction, (c) annual temperature and melt fraction where annual precipitation was less than 0.45 m/yr, (d) annual precipitation and sublimation fraction, (e) annual temperature and sublimation fraction, and (f) annual temperature and sublimation fraction where annual precipitation was less than 0.45 m/yr. Scandinavia and Baffin Island are plotted with an "S" and a "B," respectively.

configuration scenarios. To examine the effects of variations in orbital forcings on the mass balance of ice sheets in an interglacial context, we used linear reconstruction equations (Erb et al., 2015) to construct time series of ELA anomalies driven by the variations in the orbital parameters over the past 800 ky. We focused on Scandinavia and Baffin Island, where the Scandinavian and Laurentide ice sheets are thought to have originated. The conclusions from this work can be summarized as follows.
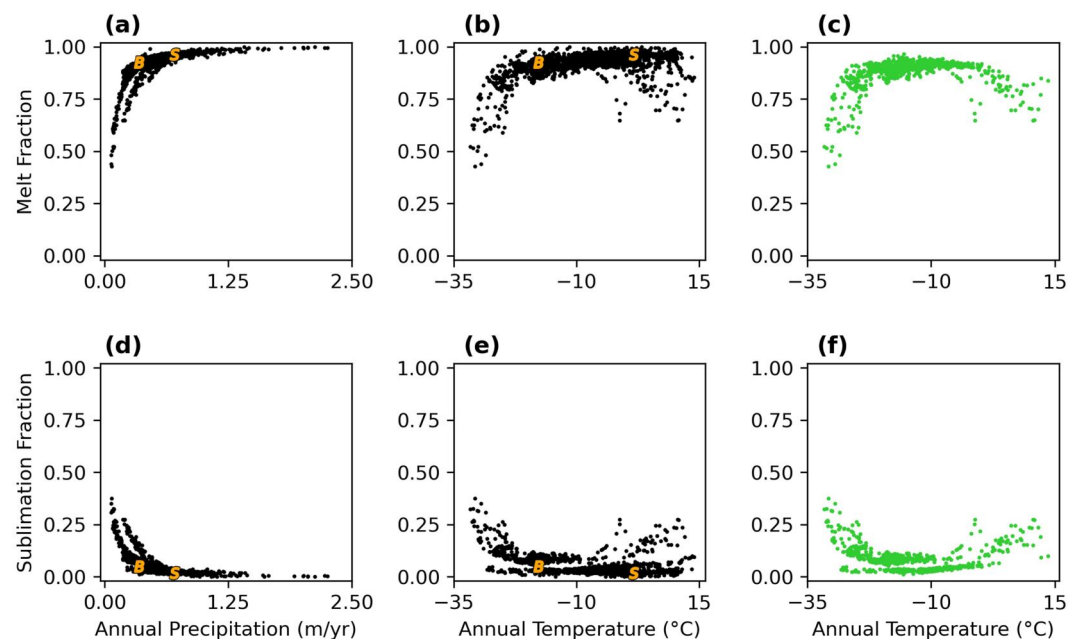


**Figure 10.** Same as Figure 9 but for National Center for Atmospheric Research.
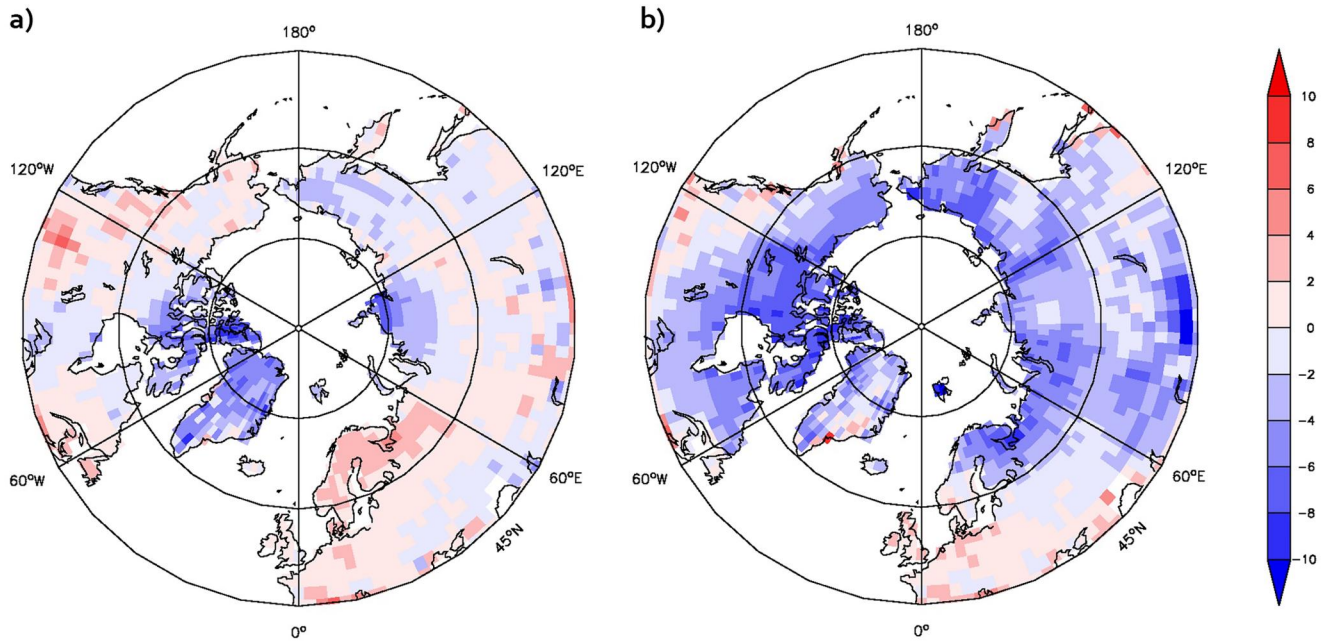
**Figure 11.** National Center for Atmospheric Research minus Geophysical Fluid Dynamics Laboratory temperature (°C) in (a) summer and (b) winter.
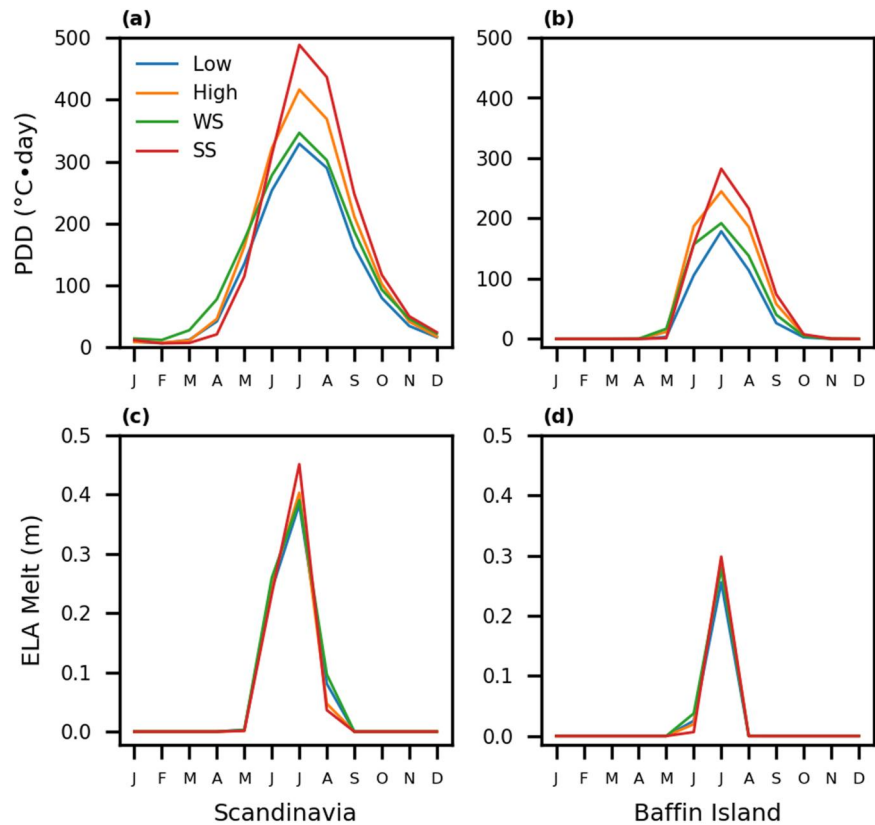


**Figure 12.** Annual distribution of (a) positive degree days (PDDs) in Scandinavia, (b) PDDs in Baffin Island, (c) equilibrium line altitude (ELA) melt in Scandinavia, and (d) ELA melt in Baffin Island for each of the Geophysical Fluid Dynamics Laboratory experiments.

- Precession was the dominant driver to ELA anomalies in Baffin Island and Scandinavia in GFDL and in Scandinavia in NCAR. Precession and obliquity played equal roles in Baffin Island in NCAR.
- The dominance of precession in GFDL contrasts with previous results which found that obliquity was somewhat more important in these regions when using PDDs as a metric for ablation (O'Neill & Broccoli, 2021). This is likely due to the difference in the monthly distribution of melt from the ELA model, which peaked sharply in July and were zero for half of the year, and PDDs, which had a broader peak and were gradually less in the adjacent months, never reaching zero.
- Differences in results between GFDL and NCAR were likely due to differences in how each model simulated temperature in their base states. NCAR has a colder polar region than GFDL, which includes Baffin Island. This resulted in ELA anomalies that were more than twice as large in Baffin Island in NCAR compared to Scandinavia and both regions in GFDL.
- Ablation was more important in determining ELA anomalies than precipitation because changes in the ELA resulting from orbital effects on precipitation alone were small in the regions of interest. The precipitation-induced changes were also often out of phase with the ELA since colder summers decrease ablation but also decrease precipitation.
- Annual ablation at land locations north of 45°N were dominated by melt. Locations with colder temperatures and less precipitation had a larger fraction of ablation come from sublimation than warmer, wetter locations. Baffin Island had more sublimation than Scandinavia since its climate is drier and colder than that of Scandinavia.

The focus of this study has been to understand how orbital variations would make the climate more or less conducive to high-latitude glaciation in a somewhat idealized context. One simplification is that the obliquity and precession simulations represent perturbations around an interglacial climate. Accordingly, the results are more relevant to mechanisms of glacial inception, for which the starting point is an interglacial state. Although the effects of "fast" climate feedbacks (albedo, water vapor, clouds, etc.) are incorporated in the climate models and therefore influence the ELA responses, the reconstructions of temporal variations in ELA do not include the important feedbacks involving atmospheric composition or ice sheet growth and decay.

The results presented herein do not address how the ELA would respond to dynamical influences that result from ice sheet growth and decay. In that sense, this paper describes a sensitivity study rather than an attempt to simulate the full response of the climate system including ice sheet-climate interactions. A more complete understanding of the mechanisms that drive glacial-interglacial variations will require experiments that couple climate models and ice sheet models (e.g., Smith et al., 2021) and address the challenges associated with the different time scales that characterize these components of the climate system.

## Data Availability Statement

The GFDL CM2.1 model output are available from Erb, Broccoli, and Raney (2018). The NCAR CESM output are available from Erb, Jackson, and DiNezio (2018). The orbital parameter data is available from Berger and Loutre (1999).

## References

Bajo, P., Drysdale, R. N., Woodhead, J. D., Hellstrom, J. C., Hodell, D., Ferretti, P., et al. (2020). Persistent influence of obliquity on ice age terminations since the Middle Pleistocene transition. *Science*, *367*(6483), 1235–1239. https://doi.org/10.1126/science.aaw1114

Barker, S., Starr, A., van der Lubbe, J., Doughty, A., Knorr, G., Conn, S., et al. (2022). Persistent influence of precession on northern ice sheet variability since the early Pleistocene. *Science*, *376*(6596), 961–967. https://doi.org/10.1126/science.abm4033

Berger, A., & Loutre, M. F. (1991). Insolation values for the climate of the last 10 million years. *Quaternary Science Reviews*, *10*(4), 297–317. https://doi.org/10.1016/0277-3791(91)90033-q

Berger, A., & Loutre, M. F. (1999). Parameters of the Earths orbit for the last 5 million years in 1 kyr resolution [Dataset]. *PANGAEA*. https://doi.org/10.1594/PANGAEA.56040

Braithwaite, R. J. (1995). Positive degree-day factors for ablation on the Greenland ice-sheet studied by energy-balance modeling. *Journal of Glaciology*, *41*(137), 153–160. https://doi.org/10.3189/S0022143000017846

Crucifix, M., & Loutre, M. F. (2002). Transient simulations over the last interglacial period (126-115 kyr BP): Feedback and forcing analysis. *Climate Dynamics*, *19*(5–6), 417–433. https://doi.org/10.1007/s00382-002-0234-z

Delworth, T. L., Broccoli, A. J., Rosati, J., Stouffer, R. J., Balaji, V., Beesley, J. A., et al. (2006). GFDL's CM2 global coupled climate models. Part I: Formulation and simulation characteristics. *Journal of Climate*, *19*(5), 643–674. https://doi.org/10.1175/jcli3629.1

Dong, B., & Valdes, P. J. (1995). Sensitivity studies of northern hemisphere glaciation using an atmospheric general circulation model. *Journal of Climate*, *8*(10), 2471–2496. https://doi.org/10.1175/1520-0442(1995)008<2471:ssonhg>2.0.co;2

Erb, M., Broccoli, A., & Raney, B. (2018). Idealized single-forcing GCM simulations with GFDL CM2.1 (Version 1) [Dataset]. *Zenodo*. https://doi.org/10.5281/zenodo.1194480

Erb, M., Jackson, C., & DiNezio, P. (2018). Idealized single-forcing GCM simulations with NCAR CESM (Version 1) [Dataset]. *Zenodo*. https://doi.org/10.5281/zenodo.1194490

Erb, M. P., Broccoli, A. J., & Clement, A. C. (2013). The contribution of radiative feedbacks to orbitally driven climate change. *Journal of Climate*, *26*(16), 5897–5914. https://doi.org/10.1175/JCLI-D-12-00419.1

Erb, M. P., Jackson, C. S., & Broccoli, A. J. (2015). Using single-forcing GCM simulations to reconstruct and interpret quaternary climate change. *Journal of Climate*, *28*(24), 9746–9767. https://doi.org/10.1175/jcli-d-15-0329.1

Erb, M. P., Jackson, C. S., Broccoli, A. J., Lea, D. W., Valdes, P. J., Crucifix, M., & DiNezio, P. N. (2018). Model evidence for a seasonal bias in Antarctic ice cores. *Nature Communications*, *9*(1), 1361. https://doi.org/10.1038/s41467-018-03800-0

Gildor, H., & Tziperman, E. (2001). A sea ice climate switch mechanism for the 100-kyr glacial cycles. *Journal of Geophysical Research*, *106*(C5), 9117–9133. https://doi.org/10.1029/1999JC000120

Hays, J. D., Imbrie, J., & Shackleton, N. J. (1976). Variations in the Earth's orbit: Pacemaker of the ice ages. *Science*, *194*(4270), 1121–1132. https://doi.org/10.1126/science.194.4270.1121

Hurrell, J. W., Holland, M. M., Gent, P. R., Ghan, S., Kay, J. E., Kushner, P. J., et al. (2013). The community Earth system model: A framework for collaborative research. *Bulletin America Meteorology Social*, *94*(9), 1339–1360. https://doi.org/10.1175/bams-d-12-00121.1

Huybers, P. (2006). Early Pleistocene glacial cycles and the integrated summer insolation forcing. *Science*, *313*(5786), 508–511. https://doi.org/10.1126/science.1125249

Huybers, P., & Tziperman, E. (2008). Integrated summer insolation forcing and 40,000-year glacial cycles: The perspective from an ice-sheet/energy-balance model. *Paleoceanography*, *23*(1), PA1208. https://doi.org/10.1029/2007pa001463

Huybers, P., & Wunsch, C. (2005). Obliquity pacing of the late Pleistocene glacial terminations. *Nature*, *434*(7032), 491–494. https://doi.org/10.1038/nature03401

Imbrie, J., Hays, J. D., Martinson, D. G., McIntyre, A., Mix, A. C., Morley, J. J., et al. (1984). The orbital theory of Pleistocene climate: Support from a revised chronology of the marine $\delta^{18}O$ record. *Milankovitch and Climate, Part*, *1*, 269–305.

Jackson, C. S., & Broccoli, A. J. (2003). Orbital forcing of Arctic climate: Mechanisms of climate response and implications for continental glaciation. *Climate Dynamics*, *21*(7–8), 539–557. https://doi.org/10.1007/s00382-003-0351-3

Kayastha, R. B., Ohata, T., & Ageta, Y. (1999). Application of a mass-balance model to a Himalayan glacier. *Journal of Glaciology*, *45*(151), 559–567. https://doi.org/10.3189/S002214300000143X

Khodri, M., Cane, M. A., Kukla, G., Gavin, J., & Braconnot, P. (2005). The impact of precession changes on the Arctic climate during the last interglacial–glacial transition. *Earth and Planetary Science Letters*, *236*(1–2), 285–304. https://doi.org/10.1016/j.epsl.2005.05.011

Lee, S.-Y., & Poulson, C. J. (2008). Amplification of obliquity forcing through mean annual and seasonal atmospheric feedbacks. *Climate of the Past*, *4*, 205–213. https://doi.org/10.5194/cp-4-205-2008

Loutre, M.-F., Paillard, D., Vimeux, F., & Cortijo, E. (2004). Does mean annual insolation have the potential to change the climate? *Earth and Planetary Science Letters*, *22*(1–4), 1–14. https://doi.org/10.1016/s0012-821x(04)00108-6

Mantsis, D. F., Clement, A. C., Broccoli, A. J., & Erb, M. P. (2011). Climate feedbacks in response to changes in obliquity. *Journal of Climate*, *24*(11), 2830–2845. https://doi.org/10.1175/2010jcli3986.1

Mantsis, D. F., Lintner, B. R., Broccoli, A. J., Erb, M. P., Clement, A. C., & Park, H. S. (2014). The response of large-scale circulation to obliquity-induced changes in meridional heating gradients. *Journal of Climate*, *27*(14), 5504–5516. https://doi.org/10.1175/jcli-d-13-00526.1

Maslin, M. A., & Ridgwell, A. J. (2005). *Mid-Pleistocene revolution and the 'eccentricity myth'* (Vol. 247, pp. 19–34). Geological Society, London, Special Publications. https://doi.org/10.1144/GSL.SP.2005.247.01.02

Milankovitch, M. (1998). Canon of insolation and the ice-age problem. In *Belgrade:Zavod za udzbenike i nastavna sredstva. (Originally published by the Royal Serbian Academy as Kanon der Erdbestrahlung und seine Anwendung auf das Eiszeitenproblem)* (Vol. 1941). Mihalia Curcica.

O'Neill, G. R., & Broccoli, A. J. (2021). Orbital influences on conditions favorable for glacial inception. *Geophysical Research Letters*, *48*(21). https://doi.org/10.1029/2021GL094290

Pisias, N. G., & Moore, T. C., Jr. (1981). The evolution of Pleistocene climate: A time series approach. *Earth and Planetary Science Letters*, *52*(2), 450–458. https://doi.org/10.1016/0012-821x(81)90197-7

Pollard, D., & Reusch, D. B. (2002). A calendar conversion method for monthly mean paleoclimate model output with orbital forcing. *Journal of Geophysical Research*, *107*(D22), 4615–4621. https://doi.org/10.1029/2002jd002126

Raymo, M. E., & Nisancioglu, K. (2003). The 41 kyr world: Milankovitch's other unsolved mystery. *Paleoceanography*, *18*(1), 1011–1017. https://doi.org/10.1029/2002pa000791

Ridgwell, A. J., Watson, A. J., & Raymo, M. E. (1999). Is the spectral signature of the 100 kyr glacial cycle consistent with a Milankovitch origin? *Paleoceanography*, *14*(4), 437–440. https://doi.org/10.1029/1999pa900018

Ruddiman, W. F., Raymo, M. E., Martinson, D. G., Clement, B. M., & Backman, J. (1989). Pleistocene evolution: Northern hemisphere ice sheets and North Atlantic ocean. *Paleoceanography*, *4*, 353–412. https://doi.org/10.1029/pa004i004p00353

Rupper, S., & Roe, G. (2008). Glacier changes and regional climate: A mass and energy balance approach. *Journal of Climate*, *21*(20), 5384–5401. https://doi.org/10.1175/2008JCLI2219.1

Smith, R. S., George, S., & Gregory, J. M. (2021). FAMOUS version xotzt (FAMOUS-ice): A general circulation model (GCM) capable of energy- and water-conserving coupling to an ice sheet model. *Geoscientific Model Development*, *14*(9), 5769–5787. https://doi.org/10.5194/gmd-14-5769-2021

Tabor, C. R., Poulsen, C. J., & Pollard, D. (2014). Mending Milankovitch's theory: Obliquity amplification by surface feedbacks. *Climate of the Past*, *10*(1), 41–51. https://doi.org/10.5194/cp-10-41-2014

## Erratum

The originally published version of this article contained typographical errors. The captions for panels (b) and (c) in Figures 4 and 7 were swapped. The caption for Figure 4 should read as follows: "Ranges (in meters) of component equilibrium line altitude time series of (a) Geophysical Fluid Dynamics Laboratory (GFDL) obliquity, (b) GFDL precession, (c) National Center for Atmospheric Research (NCAR) obliquity, and (d) NCAR precession." The caption for Figure 7 should read as follows: "Map of ranges of ablation-only time series (in meters)

for (a) Geophysical Fluid Dynamics Laboratory (GFDL) obliquity, (b) GFDL precession, (c) National Center for Atmospheric Research (NCAR) obliquity, and (d) NCAR precession, at the precession phasing that maximizes the effect of precession on the equilibrium line altitude." The errors have been corrected, and this may be considered the authoritative version of record.